

Tuning the Thermoresponse Properties of Weak Polyelectrolytes: Aqueous Solutions of Star-Shaped and Linear Poly(*N,N*-dimethylaminoethyl Methacrylate)

Felix A. Plamper,[†] Markus Ruppel,[†] Alexander Schmalz,[†] Oleg Borisov,[‡] Matthias Ballauff,^{*,§} and Axel H. E. Müller^{*,†}

Makromolekulare Chemie II, Physikalische Chemie I, and Bayreuther Zentrum für Kolloide und Grenzflächen, Universität Bayreuth, D-95440 Bayreuth, Germany, and Institut Pluridisciplinaire de Recherche sur l'Environnement et les Matériaux, UMR 5254 CNRS/UPPA, 64053 Pau, France

Received May 28, 2007; Revised Manuscript Received September 3, 2007

ABSTRACT: We investigated the thermoresponse behavior of aqueous solutions of star-shaped and linear poly(*N,N*-dimethylaminoethyl methacrylate) (PDMAEMA). The observed cloud points strongly decrease with increasing pH of the solution. This is explained by a weak charging of the star polymers with decreasing pH. A significant decrease of the cloud points with increasing molecular weight for high pH, i.e., for the almost uncharged state, was found to be virtually independent of the arm number and arm length. These findings are explained by classical Flory–Huggins theory. The increase of cloud points upon charging is captured by introduction of an effective degree of polymerization. Polymers with shorter arms show slightly higher cloud points at low pH than polymers with longer arms. The intramolecular segment density also influences the observed apparent pK_b values, leading to higher values for stars with higher arm numbers.

Introduction

Thermoresponse polymers, which show a pronounced change in their solvation at a certain temperature, caused much attention in former research. Especially thermoresponse polymers, which are water-soluble, are of interest in respect to applications under physiological conditions.^{1–5} These polymers show partial solubility in a certain temperature range, whereas full solubility is accomplished outside the temperature range. Hereby the binodal line separates the one-phase region from the two-phase region. A maximum in the coexistence curve accounts for the upper critical solution temperature (UCST), whereas a minimum in the binodal represents the lower critical solution temperature (LCST). For LCST polymers, the phase separation at higher temperatures is owing to an entropy loss due to ordering of solvent molecules around the polymer segments.

The cloud points (single point on the binodal) of thermosensitive polymer solutions are believed to be influenced by the architecture of the polymer.⁶ Theoretical considerations predicted a stabilization against phase separation by branching.^{7–9} For an organosoluble star-like polymer (polystyrene in cyclohexane), there is experimental evidence that the one-phase region becomes extended upon an increase in the degree of branching (lowering of the UCST).^{10,11} However, experimental data do not give a uniform picture for water-soluble LCST polymers.

One of the most prominent LCST polymers is poly(*N*-isopropylacrylamide) (PNIPAAm) which usually shows a LCST around 32 °C in water.^{12,13} Though there is still some controversy regarding the molecular weight dependence of the

LCST,^{14,15} PNIPAAm is regarded to belong to the so-called class II of LCST polymers (according to Berghmans' classification).^{16,17} That means the observed LCST is hardly dependent on the molar mass of the polymer. Architecture has negligible effect as well, since star-shaped PNIPAAm does not change its LCST compared to the linear polymer.¹⁸ Exceptions are given by polymers with hydrophobic/hydrophilic endgroups^{14,19,20} and polymers with a high number of arms (high arm number prevents macroscopic demixing under microscopic collapse).^{17,21} Also other architectures of PNIPAAm show the transition to bad solvent conditions around 32 °C (e.g., spherical brushes).^{22,23}

Another example of LCST-polymers is poly(*N,N*-dimethylaminoethyl methacrylate) (PDMAEMA). However, the cloud points of the latter polymer reported in literature vary from 14 to 50 °C in pure water (46 °C in pH 7 buffer).^{24–28} This gives some indication of a class I LCST behavior (LCST depends on molecular weight). Patrickios and co-workers investigated the thermoresponse properties of PDMAEMA stars, which were prepared by the arm-first method. Thus they have larger hydrophobic cores.²⁹ They report that the cloud point in pure water does not depend much on the arm number (a change from 29 °C for a star with 24 arms to 34 °C for a star with 50 arms was observed). PDMAEMA brushes were prepared by Matyjaszewski et al.³⁰ They copolymerized a minor amount of a light-sensitive azobenzene monomer to investigate the observed cloud points in dependence of illumination. The brushes with *cis*-azobenzene units did not show any macroscopic demixing, whereas the brush with *trans*-azobenzene units showed a moderate decrease in transmission at rather high concentration (1 wt %). These examples imply the conclusion that macroscopic phase separation is hampered for thermoresponse polymers with higher branching and/or segment densities. The result that phase separation is prevented for PNIPAAm brushes or PNIPAAm stars with high arm number supports this conclusion.^{21–23} One possible reason is given in the review of Aseyev et al.¹⁷ Aggregation is kinetically prevented for even linear

* To whom correspondence should be addressed. E-mail: matthias.ballauff@uni-bayreuth.de (M.B.); axel.mueller@uni-bayreuth.de (A.H.E.M.). Fax: +49-921-553393.

[†] Makromolekulare Chemie II and Bayreuther Zentrum für Kolloide und Grenzflächen, Universität Bayreuth.

[‡] UMR 5254 CNRS/UPPA.

[§] Physikalische Chemie I and Bayreuther Zentrum für Kolloide und Grenzflächen, Universität Bayreuth.

Table 1. Experimental Conditions for the Synthesis of Linear PDMAEMA^a

sample	[DMAEMA] ₀ (mol/L)	[initiator] ₀ (mmol/L)	[CuBr] (mmol/L)	[CuBr ₂] (mmol/L)	<i>t</i> (min)	conversion, <i>x_p</i> ^d
1A	1.4 ^e	5.8 ^b	4.9	1.0	180	0.26
1B	1.4 ^e	5.8 ^b	4.9	1.0	600	0.38
1C	5.9 ^f	10 ^c			20	0.08
1D	5.9 ^f	1 ^c			120	0.16

^a *T* = 60 °C. ^b Initiator: ethyl- α -bromoisobutyrate EBIB. ^c Initiator: azobisisobutyronitrile (AIBN). ^d Determined by NMR. ^e Solvent: anisole. ^f Performed in bulk.

Table 2. Number-Average Degrees of Polymerization of Linear PDMAEMA and Polydispersities (in Parentheses; Both Obtained by Different Methods), Initiation Site Efficiencies, *f_i*, Derived Therefrom (Bold, Italic), and the Resulting Formulas: PDMAEMA_{*n*} (*n* Equals Number-Average Degree of Polymerization)

	1A	1B	1C	1D
GPC of linear PMAA	126 (1.18); 0.52	155 (1.23); 0.62	1590 (6.5)	1740 (5.3)
GPC of linear PMMA	105 (1.06); 0.62	134 (1.10); 0.72	1270 (1.9)	1470 (1.8)
MALDI of PMMA	100(1.10); 0.65	115 (1.16); 0.83		
average	0.60	0.72		
approximate formula	PDMAEMA ₁₀₈	PDMAEMA ₁₃₃	PDMAEMA ₁₄₀₀	PDMAEMA ₁₆₀₀

polymers especially at low particle concentrations due to vitrification of the intermediate colloidal globules.

The introduction of charges leads to an additional, effective stabilization of macromolecules in solution against aggregation and phase separation. PDMAEMA is a useful polymer to study the effects of charges on the LCST, since it is a weak cationic polyelectrolyte. The thermoresponsive properties of the polybase PDMAEMA can then be altered by slight changes in pH and salinity as well. pH and salinity do not show pronounced effects for the neutral PNIPAAm unless incorporation of ionizable groups introduces pH sensitivity.^{31–34} These modified, linear PNIPAAm polymers were studied to demonstrate the increase of the cloud points by varying the degree of ionization.

The effect of ionic charges on phase separation in polymer solution has been amply studied theoretically. Vasilevskaya et al. demonstrated that incorporation of a small fraction of permanently charged monomer units in the chain enhances the solubility and weakens the tendency for macroscopic phase separation (precipitation) due to an additional contribution of translational entropy of the counterions.³⁵ Khokhlov et al. demonstrated that the effect of weak charges can be captured to first approximation by an effective degree of polymerization $1/DP_{\text{eff}} = 1/DP + \alpha'$, where α' is the degree of dissociation. Bokias et al. have generalized the approach of Khokhlov et al. and proposed a model of “migrating charges” to explain the effect of incorporation of pH sensitive monomer units on the LCST of the modified PNIPAAm.³³ Although the latter model does not account correctly for ionization equilibrium in both dilute and concentrated polymer phases in buffered solution, it does capture the dominant effect of increasing contribution of translation entropy of the counterions upon increasing ionization provoked by the pH variation. Borue and Erukhimovich demonstrated that solutions of weakly charged polyelectrolytes exhibit a microphase separation instead of precipitation upon a decrease in the solvent strength below the θ -point.³⁶

Therefore we report on the investigation of the thermoresponsive properties of a well defined set of star-shaped PDMAEMA. The polymers were prepared by the core-first method yielding stars with up to 24 arms and rather low polydispersity (absolute PDI ≤ 1.43). In contrast, PDMAEMA stars made by arm-first methods usually exhibit higher polydispersities (e.g., $PDI_{\text{app}} > 1.6$),³⁷ possess a rather large hydrophobic core, and possess possibly hydrophobic initiator moieties attached at the periphery. These effects might alter the LCST behavior. The results are compared to those obtained with linear polymers. For details of synthesis and characterization

we refer to an earlier paper.³⁸ The present work aims at a systematic investigation of the LCST behavior of PDMAEMA. In particular, the influence of charges on the demixing temperature is studied and compared to the model of Khokhlov et al. in a semiquantitative manner.

Experimental Section

The synthesis and characterization of star-shaped PDMAEMA by ATRP using CuBr/HMTETA in anisole are described in a previous paper.³⁸ Linear PDMAEMA **1A** and **1B** were prepared according to the same recipe using ethyl- α -bromoisobutyrate (EBIB) as the initiator. The numbers in our nomenclature (1, 5, 8, 21, and 58) assign the relative number of initiation sites of the (multifunctional) initiators used for the synthesis of the (star-shaped) polymers. The letters differentiate between different batches (A, B, etc.). Longer PDMAEMA (**1C**, **1D**) was synthesized by conventional radical polymerization using AIBN (Merck) as the initiator. The monomer DMAEMA (Merck) was filtered over basic alumina; the initiator was dissolved in 10 mL of monomer before the mixture was purged with nitrogen to eliminate oxygen. The mixture was placed in oil bath, and after an appropriate time, the mixture was cooled. ¹H NMR spectroscopy (Bruker Avance 250 MHz) was performed to determine conversion.³⁸ The polymer was precipitated from hexane and finally freeze-dried from dioxane. The conditions used for the polymerizations are listed in Table 1. The characterization of all linear PDMAEMA was performed in the same way as described before;³⁸ the polymers were converted to poly(methacrylic acid) and poly(methyl methacrylate) to achieve meaningful determination of the molecular weights by gel permeation chromatography (GPC) and sometimes by matrix assisted laser desorption ionization time-of-flight (MALDI-TOF) mass spectrometry. The results are listed in Table 2. The formulas of all polymers used are listed in Table 3 ((PDMAEMA)_{*n*})_{*x*}; *n* = number-average degree of polymerization per arm; *x* = number-average arm number).

The determination of the cloud points was achieved by turbidity measurements using a titrator (Titrand 809, Metrohm, Herisau, Switzerland) equipped with a turbidity sensor ($\lambda_0 = 523$ nm, Spectrosense, Metrohm). In addition, a temperature sensor (Pt 1000, Metrohm) and a pH sensor (micro pH glass electrode, Metrohm) were used. The temperature program (1 K/min) was run by a thermostat (LAUDA RE 306 and Wintherm_Plus software), using a homemade thermostatable vessel. All aqueous solutions were prepared either from Millipore water or buffer (pH = 10, boric acid buffer Titrimorm, VWR; pH = 9, boric acid buffer 9461, Merck; pH = 8, boric acid buffer CertiPUR, Merck; pH = 7, phosphate buffer 82571, Fluka; ionic strength of all buffers in the order of 0.05 mol/L) by vigorous stirring. The solutions were degassed by applying vacuum (50–100 mbar) for 15 min at room

Table 3. Cloud Points T_{cl} of PDMAEMA under Different Conditions (1.0 g/L; *Italic*, 0.1 g/L) and $pK_{b,app}$ (Bold, $pK_{a,app}$ Measured as pH at $\alpha = 0.5$, 1.0 g/L in Pure Water and Converted into $pK_{b,app}$ Using $pK_{a,app} + pK_{b,app} = 14$)

	pH = 7	pH = 8	pH = 9	pH = 10	$pK_{b,app}$
1A PDMAEMA ₁₀₈	76.0; 79.9	53.0; 56.5	42.3; 46.9	38.7; 44.4	7.78
1B PDMAEMA ₁₃₃	78.7	54.4	43.0	40.5	7.78
1C PDMAEMA ₁₄₀₀	77.6	-	-	28.9	
1D PDMAEMA ₁₆₀₀	77.7	-	-	25.0	
5A (PDMAEMA ₁₀₀) _{3.1}	78.0	51.3	40.0	36.0	7.94
5E (PDMAEMA ₁₆₀) _{3.7}	77.0	50.0	36.9	32.6	7.98
8A (PDMAEMA ₁₁₀) _{5.4}	77.6	50.0	36.9	32.9	7.98
8E (PDMAEMA ₁₇₀) _{5.6}	77.6	49.3	35.1	31.0	7.98
21A (PDMAEMA ₁₇₀) _{9.5}	80.0	49.1	33.7	29.3	
21E (PDMAEMA ₂₄₀) ₁₁	78.0	48.7	32.7	28.0	8.05
58A (PDMAEMA ₁₇₀) ₁₈	78.7	49.1	31.1; 32.6	27.8	8.16
58E (PDMAEMA ₂₄₀) ₂₄	78.7	48.7	31.5	25.8	8.11

temperature to minimize bubble formation during heating. The solutions were measured under nitrogen for measurements without buffer. We defined the cloud point as the intercept of the tangents at the onset of turbidity (Figure 1). The potentiometric titrations (titer 0.1 N HCl 0.06 mL/min) were performed under similar conditions, using the same pH electrode (connected to a separation amplifier). Instead of a turbidity sensor, a conductivity sensor (712 Conductometer, Metrohm) was used to determine the equivalence point of the titration (intercept of tangents in the conductivity curve).

We took only freshly prepared solutions for the titrations and for all turbidity measurements. This helps to obtain reliable data, since a shift of cloud points to higher temperatures was observed during turbidity measurements when using several heating and cooling cycles (see Figure S2 in Supporting Information).

Results and Discussion

In this contribution we investigate the cloud points of aqueous solutions of star-shaped poly(dimethylaminoethyl methacrylate) (PDMAEMA) in dependence of the arm number, arm length and pH. For this reason we performed turbidity measurements applying a temperature ramp and defined the cloud point as the intercept of the tangents at the onset of turbidity. The pH dependence with temperature in buffer-free solutions shows a kink very close to this temperature (Figure 1). This indicates that the intra- and intermolecular aggregation leads to an increase in the local density of polymer and therefore hinders ionization of the amino groups. The initial slope of the pH curve is mainly determined by the change of the protonation equilibrium along with the change in the solubilizing abilities of water with temperature (electrode potential was corrected with respective temperature to obtain current pH). The protonation equilibrium is also altered by the degree of branching as seen in potentiometric titrations (Figure 2 and Figure S1 of Supporting Information) and as expected by theory.³⁹

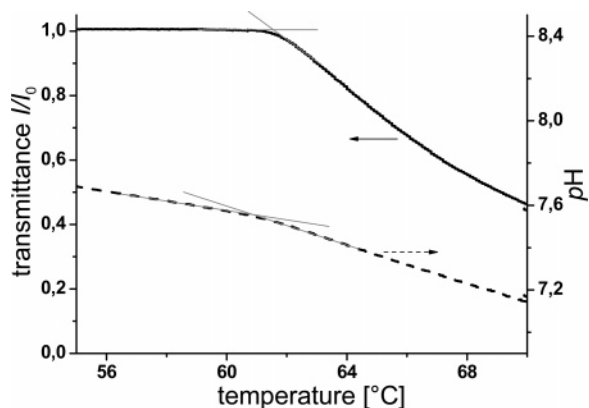


Figure 1. Determination of cloud points T_{cl} (extraction of cloud point from the turbidity data and comparison with cloud point obtained by pH measurement; here: 0.1 g/L **1A** PDMAEMA₁₀₈ in pure water).

The titration curves are shifted to lower pH values for higher arm numbers but similar arm length (e.g., compare **1A** and **8A**). That means that the apparent $pK_{b,app}$ increases with higher branching (see Table 3). $pK_{b,app} = -\log[OH^-]_{\alpha=0.5}$ is determined as $pK_w - pH_{\alpha=0.5}$, where pK_w is the negative decadic logarithm of the equilibrium constant of the autodissociation of water K_w . This result is consistent with former results found with the help of star-shaped poly(acrylic acid).⁴⁰ For this polyacid, the apparent pK_a increased with increasing branching. This was explained by the high concentration of counterions inside the branched structure, which hampers the deprotonation of the weak polyacid at the same degree of neutralization. Analogously our polybase keeps a certain amount of HCl for its own microscopic Donnan equilibrium. An increasing part of the added HCl does not contribute to the protonation of the amino groups, when the branching increases. This is again due to the increasing osmotic pressure inside the star, which opposes the protonation. For the dependence of the apparent pK_b on the arm length see Supporting Information and a previous publication.⁴⁰

Because of the considerable drop of pH during heating in pure water (Figure 1) and the anticipated effect of the pH on the LCST behavior, we primarily investigated the cloud points of the star-shaped polymers in buffer solution. This keeps the pH more constant over the whole temperature range. However at the same time, the ionic strength is increased (~ 0.05 mol/L) due to salt present in the buffer solution.

We performed most of the measurements at a concentration of 0.1 g/L (each 25 mL of freshly prepared PDMAEMA solutions) in order to save polymer. There is a concentration dependence of the cloud points as expected (we move along the binodal which has the minimum in the LCST). It leads to a

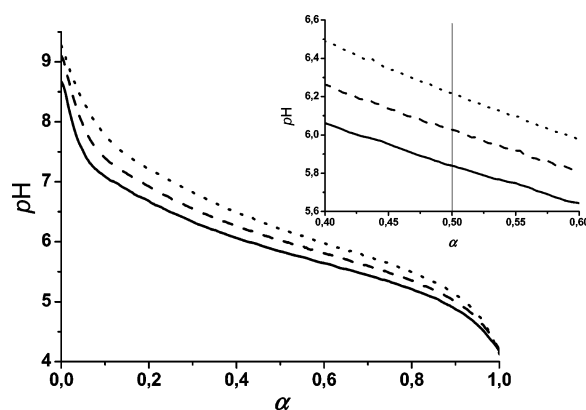


Figure 2. Titration curves of star-shaped PDMAEMA in Millipore water with 0.1 N HCl in dependence of degree of neutralization α (1.0 g/L; 24 °C; ·····, **1A** PDMAEMA₁₀₈; ---, **8A** (PDMAEMA₁₁₀)_{5.4}; —, **58A** (PDMAEMA₁₇₀)₁₈). The inset shows an enlarged portion of the graph around half neutralization.

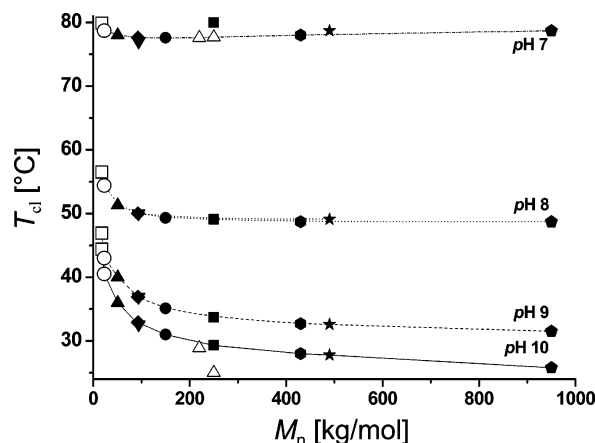


Figure 3. Cloud points, T_{cl} , at 0.1 g/L of linear and star-shaped PDMAEMA in dependence of molecular weight, M_n , (\square , PDMAEMA₁₀₈; \circ , PDMAEMA₁₃₃; \blacktriangle , (PDMAEMA₁₀₀)_{3,1}; \blacktriangledown , (PDMAEMA₁₆₀)_{3,7}; \blacklozenge , (PDMAEMA₁₁₀)_{5,4}; \bullet , (PDMAEMA₁₇₀)_{5,6}; \blacksquare , (PDMAEMA₁₇₀)_{9,5}; \bullet , (PDMAEMA₂₄₀)₁₁; \star , (PDMAEMA₁₇₀)₁₈; \bullet , (PDMAEMA₂₄₀)₂₄; \triangle , PDMAEMA₁₄₀₀ and PDMAEMA₁₆₀₀ prepared by free radical polymerization). The lines are a guide to the eye.

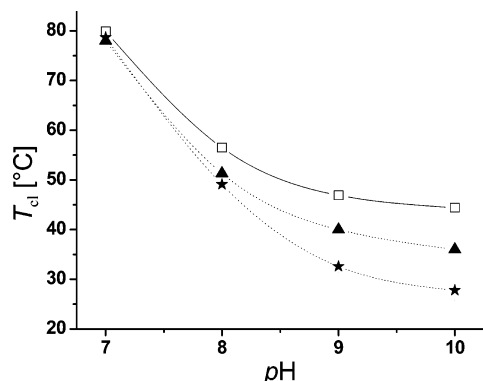


Figure 4. Cloud points T_{cl} at 0.1 g/L of linear and star-shaped PDMAEMA in dependence of pH (\square , PDMAEMA₁₀₈; \blacktriangle , (PDMAEMA₁₀₀)_{3,1}; \star , (PDMAEMA₁₇₀)₁₈).

shift of the phase boundary to lower temperatures with increasing concentration (0.1–1.0 g/L; see Table 3). The effect is more pronounced for the linear polymer, but since the effect is in the order of a few Kelvin in the investigated concentration range, we continue most of the measurements with 0.1 g/L. This is in all cases below the overlap concentration.

The cloud points at 0.1 g/L are represented in Figure 3 in dependence of molecular weight and pH (see also Figure 4).

We start the discussion at high pH (≥ 9), where the stars are almost uncharged. Here the cloud points decrease monotonously with increasing molecular weight irrespective of arm length and arm number. Therefore all cloud points seem to fit one “master curve”.

According to Flory–Huggins theory for linear polymers, the critical temperature (here T_{cl}) depends on the degree of polymerization, DP, in the following way,⁴¹

$$\frac{1}{T_{cl}} = \frac{1}{\theta} + \frac{1}{\theta\psi} \left(\frac{1}{2DP} + \frac{1}{\sqrt{DP}} \right) \quad (1)$$

θ is the theta temperature, and ψ accounts for the sign of the temperature dependence of the Flory–Huggins parameter χ . In the case of LCST polymers, $\psi < 0$. In a strict sense, eq 1 holds only true for the critical volume fraction. However, for the rather high molecular weights, the critical volume fraction is expected to be of the order of the polymer volume fractions used here.

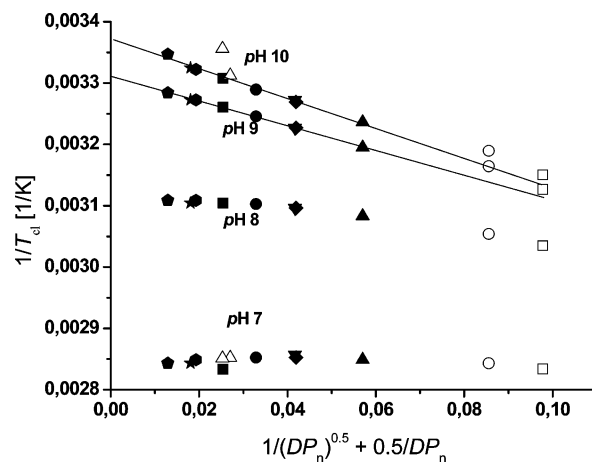


Figure 5. Plot of inverse cloud points according to Flory theory (eq 1) using the number-average degree of polymerization DP_n (\square , PDMAEMA₁₀₈; \circ , PDMAEMA₁₃₃; \blacktriangle , (PDMAEMA₁₀₀)_{3,1}; \blacktriangledown , (PDMAEMA₁₆₀)_{3,7}; \blacklozenge , (PDMAEMA₁₁₀)_{5,4}; \bullet , (PDMAEMA₁₇₀)_{5,6}; \blacksquare , (PDMAEMA₁₇₀)_{9,5}; \bullet , (PDMAEMA₂₄₀)₁₁; \star , (PDMAEMA₁₇₀)₁₈; \bullet , (PDMAEMA₂₄₀)₂₄; \triangle , PDMAEMA₁₄₀₀ and PDMAEMA₁₆₀₀ prepared by free radical polymerization).

Moreover, we only aim at a semiquantitative approach that elucidates the general trends.

Figure 5 demonstrates that the cloud points of the star-shaped polymers lie on one straight line for pH = 9 and pH = 10, respectively, in good approximation.

Slight deviations are only seen for the short linear samples. Otherwise architecture has only a negligible influence on the phase separation of the polymers studied here. Possible endgroup effects are coupled directly to architecture as the relative number of endgroups increases with arm number and decreases with arm length. Also they are not observed here and we assume that the bromine atom at the terminus does not have a significant effect on the polarity. Molecular weight alone determines the observed cloud points at constant high pH. Therefore PDMAEMA acts like an LCST polymer of class I in high pH buffer solutions.¹⁷ Even linear PDMAEMA with a rather high molecular weight (samples **1C** and **1D**, prepared by free radical polymerization) does not deviate much from the curve in Figure 3. One reason for the deviation of samples **1C** and **1D** might be the rather high polydispersity resulting from conventional radical polymerization. In conclusion, the Flory approach in terms of a temperature-dependent χ parameter seems to well describe the thermoresponsive behavior of PDMAEMA at high pH. This is in contrast to various alternative models (two-state model, n -cluster model, etc.)^{42,43} proposed to describe the LCST behavior of nonionic polymers in aqueous solutions, like, e.g., poly(ethylene oxide).⁴⁴

At decreasing pH, the PDMAEMA stars will be more and more charged (degree of neutralization $\alpha \sim 0.05$ for pH = 8 and $\alpha \sim 0.11$ –0.25 for pH = 7 in buffer-free 1 g/L solutions). This is also reflected in the shift of the phase boundary to higher temperatures as expected.^{33,45} Already at pH = 8, the cloud points increased by more than 10 K. In addition, the cloud points do not fit to one monotonous “master curve” anymore. This behavior is even more pronounced at pH = 7. Furthermore, the cloud points are now located in a rather narrow window between 77 and 80 °C, i.e., they are nearly independent of DP.

We now take into account the charging (effect of counterions) by introducing the Khokhlov concept of the “effective degree of polymerization”^{33,46}

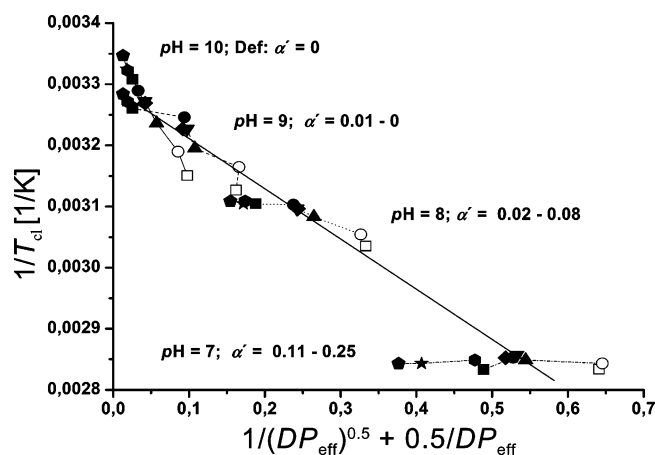


Figure 6. Cloud point data plotted according to eq 1 after introduction of the effective degree of polymerization (eq 2) (\square , PDMAEMA₁₀₈; \circ , PDMAEMA₁₃₃; \blacktriangle , (PDMAEMA₁₀₀)_{3.1}; \blacktriangledown , (PDMAEMA₁₆₀)_{3.7}; \blacklozenge , (PDMAEMA₁₁₀)_{5.4}; \bullet , (PDMAEMA₁₇₀)_{5.6}; \blacksquare , (PDMAEMA₁₇₀)_{9.5}; \bullet , (PDMAEMA₂₄₀)₁₁; \star , (PDMAEMA₁₇₀)₁₈; \blacklozenge , (PDMAEMA₂₄₀)₂₄; \triangle , PDMAEMA₁₄₀₀ and PDMAEMA₁₆₀₀ prepared by free radical polymerization).

$$DP_{\text{eff}} = \left(\frac{1}{DP} + \alpha' \right)^{-1} \quad (2)$$

where α' equals the degree of ionization. Then we can linearize the set of our cloud point data. The data points gather around one straight line when taking α (degree of neutralization) instead of α' from Figure 2 (and Figure S1 in Supporting Information). However, at low degrees of neutralization, the true degree of ionization deviates from α . This is obvious since the polymer is slightly charged ($\alpha' \neq 0$) even without any added acid ($\alpha = 0$) as seen by the basic pH of PDMAEMA solutions without buffer. The inherent salt in the buffers can alter additionally the protonation equilibrium, but even by these approximations the overall trend seems to be well-captured as seen in Figure 6. We remark that for $\alpha' DP \gg 1$, $DP_{\text{eff}} \approx 1/\alpha'$, i.e., it does not virtually depend on the actual degree of polymerization. This is in good agreement with the flattening of the LCST dependence on the DP at pH 7 and 8.

Some deviations from the master curve at high pH are caused by the small but existent charging of the polymer. A contribution to the deviations at low pH might be attributed to the architecture and the resulting counterion confinement. Moreover, at low pH the charge density (ionization) starts to have an influence on the observed cloud points. This is also seen in Figure 3: especially the polymers with shorter arms (e.g., **21A** and **58A**) show slightly higher cloud points exceeding the anticipated curve for the polymers with longer arms (e.g., **21E** and **58E**). Though higher segment density has a limited opposing effect on the ionization in salt- and buffer-free solution (see Figure 2), the increased segment density for the polymers with shorter arms leads also to an increased charge density. This may facilitate the solubility in water especially in salted and buffered solutions, where the salt-dominance regime is approached. Then the degree of ionization of monomer units is controlled by the pH imposed by the buffer solution and is virtually independent of the degree of branching.

As shown, we always get macroscopic demixing even at low concentrations of PDMAEMA in the buffer solution. Therefore, the arm number seems to be too low to prevent macroscopic phase separation as seen on PNIPAAm stars with high arm numbers.²¹ However, we do not observe macroscopic phase separation at even higher concentrations in pure water for stars with more than nine arms. In weak polyelectrolyte brushes,⁴⁷

micelles of polystyrene-*block*-poly(methacrylic acid)⁴⁸ and in micelles of poly(*n*-butyl acrylate)-*block*-poly(acrylic acid)⁴⁹ a fraction of arms collapses and forms a virtually nonionized core, whereas the other arms form an extended ionized corona. Thus, in analogy we expect that at a pH close to pK_a , a decrease in solvent strength leads to intramolecular phase separation in starlike pH-sensitive polyelectrolytes. The more strongly charged corona may efficiently prevent stars from aggregation above the LCST. This electrosteric stabilization plays the dominant role in the salt-free case. These results will be an issue of a future publication.

Conclusion

We can conclude that the cloud points of PDMAEMA in buffer solutions can be easily tuned by changing the pH, molecular weight, and concentration. At high pH, the architecture has no dominant influence on the observed cloud points. At intermediate pH it has only a minor influence of the order of a few Kelvins. Our results indicate that phase separation in PDMAEMA solutions induced by an increase in temperature can be satisfactory described following the classical Flory approach in terms of a temperature-dependent χ parameter.

Acknowledgment. We thank Andreas Walther for scientific discussions and Deutsche Forschungsgemeinschaft (DFG; Grants SFB 481 and MU896/25-1) and Fonds der Chemischen Industrie (FCI) for financial support.

Supporting Information Available: Additional titration data and stability of PDMAEMA solutions. This material is available free of charge via the Internet at <http://pubs.acs.org>.

References and Notes

- (1) Twaites, B. R.; de las Heras Alarcon, C.; Cunliffe, D.; Lavigne, M.; Pennadam, S.; Smith, J. R.; Gorecki, D. C.; Alexander, C. *J. Controlled Release* **2004**, *97*, 551–566.
- (2) Pennadam, S. S.; Ellis, J. S.; Lavigne, M. D.; Gorecki, D. C.; Davies, M. C.; Alexander, C. *Langmuir* **2007**, *23*, 41–49.
- (3) Kwon, I. K.; Matsuda, T. *Biomaterials* **2006**, *27*, 986–995.
- (4) Carter, S.; Rimmer, S.; Rutkaite, R.; Swanson, L.; Fairclough, J. P. A.; Sturdy, A.; Webb, M. *Biomacromolecules* **2006**, *7*, 1124–1130.
- (5) Wei, H.; Zhang, X.; Cheng, C.; Cheng, S.-X.; Zhuo, R.-X. *Biomaterials* **2007**, *28*, 99–107.
- (6) Russell, T. P.; Fetters, L. J.; Clark, J. C.; Bauer, B. J.; Han, C. C. *Macromolecules* **1990**, *23*, 654–659.
- (7) Zhulina, E. B.; Borisov, O. V.; Birshtein, T. M. *Vysokomol. Soedin., Ser. A* **1988**, *30*, 774–781.
- (8) Garas, G.; Kosmas, M. *Macromolecules* **1994**, *27*, 6671–6672.
- (9) Francois, J.; Beaudoin, E.; Borisov, O. *Langmuir* **2003**, *19*, 10011–10018.
- (10) Numasawa, N.; Okada, M. *Polym. J.* **1999**, *31*, 99–101.
- (11) Shmakov, S. L. *Polymer* **2001**, *43*, 1491–1495.
- (12) Taylor, L. D.; Cerankowski, L. D. *J. Polym. Sci., Part A: Polym. Chem.* **1975**, *13*, 2551–2570.
- (13) Schild, H. G. *Prog. Polym. Sci.* **1992**, *17*, 163–249.
- (14) Xia, Y.; Burke, N. A. D.; Stöver, H. D. H. *Macromolecules* **2006**, *39*, 2275–2283.
- (15) Xia, Y.; Yin, X.; Burke, N. A. D.; Stöver, H. D. H. *Macromolecules* **2005**, *38*, 5937–5943.
- (16) Meeussen, F.; Nies, E.; Berghmans, H.; Verbrugghe, S.; Goethals, E.; Du Prez, F. *Polymer* **2000**, *41*, 8597–8602.
- (17) Aseyev, V. O.; Tenhu, H.; Winnik, F. M. *Adv. Polym. Sci.* **2006**, *196*, 1–85.
- (18) Zheng, Q.; Pan, C.-Y. *Eur. Polym. J.* **2006**, *42*, 807–814.
- (19) Plummer, R.; Hill, D. J. T.; Whittaker, A. K. *Macromolecules* **2006**, *39*, 8379–8388.
- (20) Schilli, C. M.; Müller, A. H. E.; Rizzardo, E.; Thang, S. H. RAFT Polymers: Novel Precursors for Polymer-Protein Conjugates. In *Advances in Controlled/Living Radical Polymerization*; Matyjaszewski, K., Ed. ACS Symposium Series 854; American Chemical Society: Washington, DC, 2003; p 603.
- (21) Luo, S.; Xu, J.; Zhu, Z.; Wu, C.; Liu, S. *J. Phys. Chem. B* **2006**, *110*, 9132–9139.

- (22) Lu, Y.; Wittemann, A.; Ballauff, M.; Drechsler, M. *Macromol. Rapid Commun.* **2006**, *27*, 1137–1141.
- (23) Deike, I.; Ballauff, M.; Willenbacher, N.; Weiss, A. *J. Rheol.* **2001**, *45*, 709–720.
- (24) Cho, S. H.; Jhon, M. S.; Yuk, S. H.; Lee, H. B. *J. Polym. Sci., Part B: Polym. Phys.* **1997**, *35*, 595–598.
- (25) Liu, Q.; Yu, Z.; Ni, P. *Colloid Polym. Sci.* **2004**, *282*, 387–393.
- (26) Bütün, V.; Armes, S. P.; Billingham, N. C. *Polymer* **2001**, *42*, 5993–6008.
- (27) Burillo, G.; Bucio, E.; Arenas, E.; Lopez, G. P. *Macromol. Mater. Eng.* **2007**, *292*, 214–219.
- (28) Fournier, D.; Hoogenboom, R.; Thijs, H. M. L.; Paulus, R. M.; Schubert, U. S. *Macromolecules* **2007**, *40*, 915–920.
- (29) Georgiou, T. K.; Vamvakaki, M.; Patrickios, C. S.; Yamasaki, E. N.; Phylactou, L. A. *Biomacromolecules* **2004**, *5*, 2221–2229.
- (30) Lee, H.-i.; Pietrasik, J.; Matyjaszewski, K. *Macromolecules* **2006**, *39*, 3914–3920.
- (31) Pei, Y.; Chen, J.; Yang, L.; Shi, L.; Tao, Q.; Hui, B.; Li, J. *J. Biomater. Sci., Polym. Ed.* **2004**, *15*, 585–594.
- (32) Erbil, C.; Akpınar, F. D.; Uyanik, N. *Macromol. Chem. Phys.* **1999**, *200*, 2448–2453.
- (33) Bokias, G.; Vasilevskaya, V. V.; Iliopoulos, I.; Hourdet, D.; Khokhlov, A. R. *Macromolecules* **2000**, *33*, 9757–9763.
- (34) Yoo, M. H.; Sung, Y. K.; Cho, C. S.; Lee, Y. M. *Polymer* **1997**, *38*, 2759–2765.
- (35) Grosberg, A. Y.; Khokhlov, A. R., *Statistical Physics of Macromolecules*; AIP Press: New York, 1994.
- (36) Borue, V. Y.; Erukhimovich, I. Y. *Macromolecules* **1988**, *21*, 3240–3249.
- (37) Vamvakaki, M.; Patrickios, C. S. *Chem. Mater.* **2002**, *14*, 1630–1638.
- (38) Plamper, F.; Schmalz, A.; Penott-Chang, E.; Jusufi, A.; Ballauff, M.; Müller, A. *Macromolecules* **2007**, *40*, 5689–5697.
- (39) Wolterink, J. K.; van Male, J.; Stuart, M. A. C.; Koopal, L. K.; Zhulina, E. B.; Borisov, O. V. *Macromolecules* **2002**, *35*, 9176–9190.
- (40) Plamper, F. A.; Becker, H.; Lanzendörfer, M.; Patel, M.; Wittemann, A.; Ballauff, M.; Müller, A. H. E. *Macromol. Chem. Phys.* **2005**, *206*, 1813–1825.
- (41) Shultz, A. R.; Flory, P. J. *J. Am. Chem. Soc.* **1952**, *74*, 4760–4767.
- (42) Sevick, E. M. *Macromolecules* **1998**, *31*, 3361–3367.
- (43) De Gennes, P. G. *C. R. Acad. Sci., Ser. IIb* **1991**, *313*, 1117–1122.
- (44) Halperin, A. *Eur. Phys. J. B* **1998**, *3*, 359–364.
- (45) Kudlay, A. N.; Erukhimovich, I. Y.; Khokhlov, A. R. *Macromolecules* **2000**, *33*, 5644–5654.
- (46) De Gennes, P. G. *Scaling Concepts in Polymer Physics*; Cornell University Press: Ithaca, NY, 1979.
- (47) Pryamitsyn, V. A.; Leermakers, F. A. M.; Fleer, G. J.; Zhulina, E. B. *Macromolecules* **1996**, *29*, 8260–8270.
- (48) Stepanek, M.; Prochazka, K.; Brown, W. *Langmuir* **2000**, *16*, 2502–2507.
- (49) Colombani, O.; Ruppel, M.; Burkhardt, M.; Drechsler, M.; Schumacher, M.; Gradzielski, M.; Schweins, R.; Müller, A. H. E. *Macromolecules* **2007**, *40*, 4351–4362.

MA071203B